LA-UR-11-00206

Approved for public release;
distribution is unlimited.

Title:	Axis-I Diode Simulations I: Standard 2-inch cathode
Author(s):	Carl Ekdahl
Intended for:	DARHT Tech Note

Form 836 (7/06)

Axis-I Diode Simulations I: Standard 2-inch cathode

Carl Ekdahl

The standard configuration of the DARHT Axis-I diode features a 5.08-cm diameter velvet emitter mounted in the flat surface of the cathode shroud. The surface of the velvet is slightly recessed ~2.5 mm. This configuration produces a 1.75 kA beam when a 3.8-MV pulse is applied to the anode-cathode (AK) gap. This note addresses some of the physics of this diode through the use of finite-element simulations.

I. Simulations

The TRAK ray-tracing, electron gun code [1] was used to simulate the DARHT Axis-1 diode. TRAK requires an electrostatic solution for the diode region and a map of the static magnetic field. These were obtained using the finite-element field solvers ESTAT and PERMAG [2].

Electrostatic field

The electrostatic solution was based on an accurate model of the DARHT Axis-1 diode and insulator that was constructed to inform insulator repairs. I reduced this to more tractable model by eliminating unnecessary details (insulators, grading rings, etc). I also rezoned the mesh to provide more detail in the region of cathode emission, and added the details of the velvet cathode. Figure 1 shows the original model with the region of the refined model shown by heavy dashed lines.

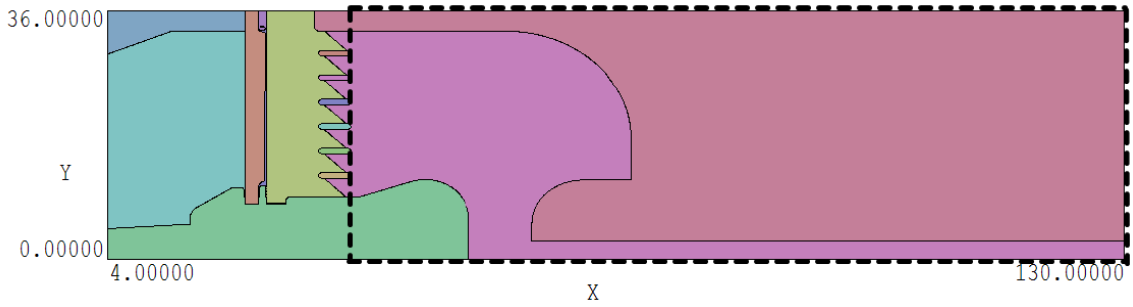

Figure 1: Full model of the DARHT Axis-1 diode and insulator region. The refined model region is outlined. Dimensions are in inches.

To simulate the electric field with no electron beam a negative potential was applied to the center conductor, reported herein as the AK voltage (unsigned). The resulting electrostatic potentials with no beam are shown in Fig. 2 for V_{AK}=3.8 MV. The potential solutions for the two models differ by less than 0.1% in the AK gap.

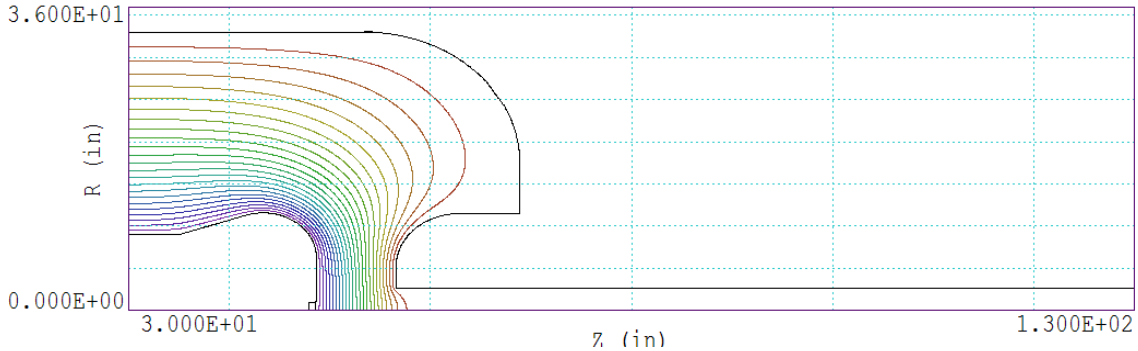

Figure 2: Electrostatic potential in the DARHT Axis-1 diode with no beam present, and V_{AK}=3.8 MV.

Figure 3 shows a blowup of the equipotentials in the emitter region. Recessing the surface of the emitter reduces the electric field at the surface to 185 kV/cm from the 208 kV/cm on the flat face of the shroud when V_{AK}=3.8 MV.

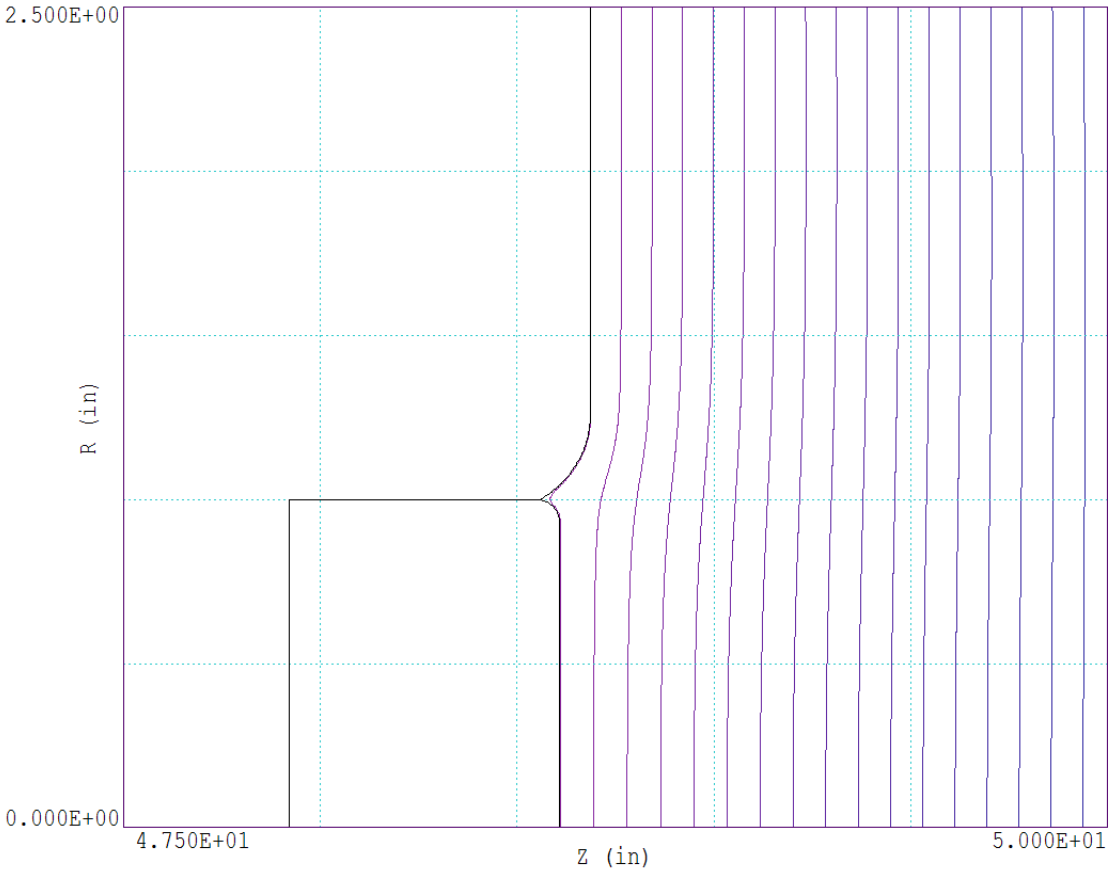

Figure 3: Close-up of the velvet emitter region with no beam. The emission surface is recessed 2.0 mm from the surface of the shroud. The electrostatic field at the surface of the emitter is 185 kV/cm compared with 208 kV/cm at the surface of the shroud when V_{AK}=3.8 MV.

External magnetic field

The magnetic field map was obtained by modeling the bucking coil and anode solenoid as ideal sheet solenoids having the dimensions and locations specified by the XTR envelope code used to tune Axis-1 [3]. The base-case field was simulated for 100 A energizing the anode solenoid and -14.51 A energizing the bucking coil. (The ratio of these two currents, k_{buck}=0.1451, was determined by inspection of current read-backs from several days of operation.) Figure 4 shows a comparison of the axial magnetic field on axis calculated using this simulation and the magnetic field calculated with the XTR models. These simulations give nearly identical results, and since the XTR models are based on field measurements, the magnetic field in these TRAK simulations is presumably in agreement with reality. The field for other anode settings (with fixed k_{buck} =0.1451) is simply obtained by scaling the base-case 100-A solution.

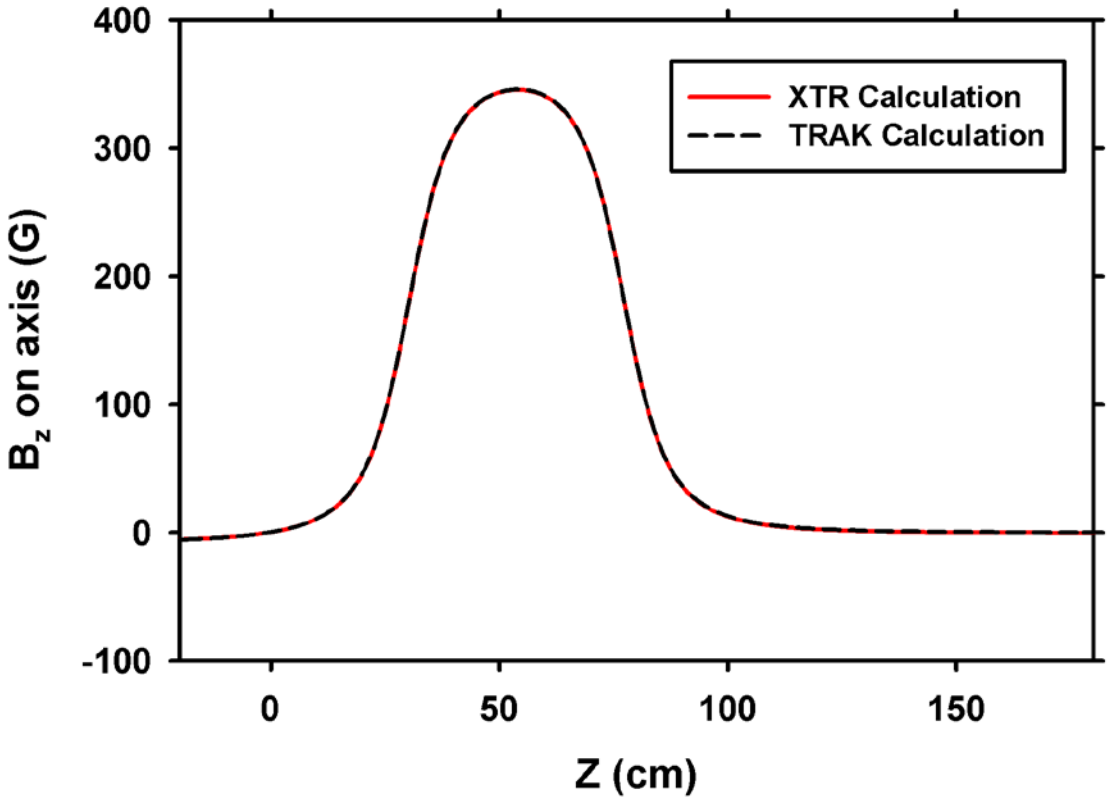

Figure 4: Axial magnetic field calculated on axis by XTR (red, solid curve) and for TRAK (black, dashed curve) for a 100-Ampere driving current on the anode solenoid, and k_{buck}=0.1451.

Space-charge limited current

Velvet cold-cathode emitters produce a plasma surface by the explosive emission process from which a space-charge limited current can be drawn [4,5,6]. Therefore, for these simulations I modeled the 2-inch diameter velvet cathode as a space-charge limited (SCL) emission surface. Space-charge limited flow of electrons can result from any source of electrons – thermionic, field emission, plasma extraction, photo-emission, or Compton scattering. The maximum current that can be drawn from any of these sources is limited by the space charge of the resulting beam. Excess electrons from the source are reflected back to the emission surface by the space-charge potential well.

High-current, flat cathodes produce beams with a lower current density at the center than at the edge. This is because the field is lower at the beam center than at the edge due to the beam space charge. Indeed, it was to overcome this effect that J. R. Pierce developed electron-gun designs with conical electrodes to flatten the equipotentials in the beam, which would otherwise be curved by space charge [7]. This effect can be clearly seen in TRAK simulations of an ideal flat emission surface. Figure 5 shows the space-charge limited beam extracted from a flat emission surface that is flush with the Axis-I shroud with V_{AK}=3.8 MV.

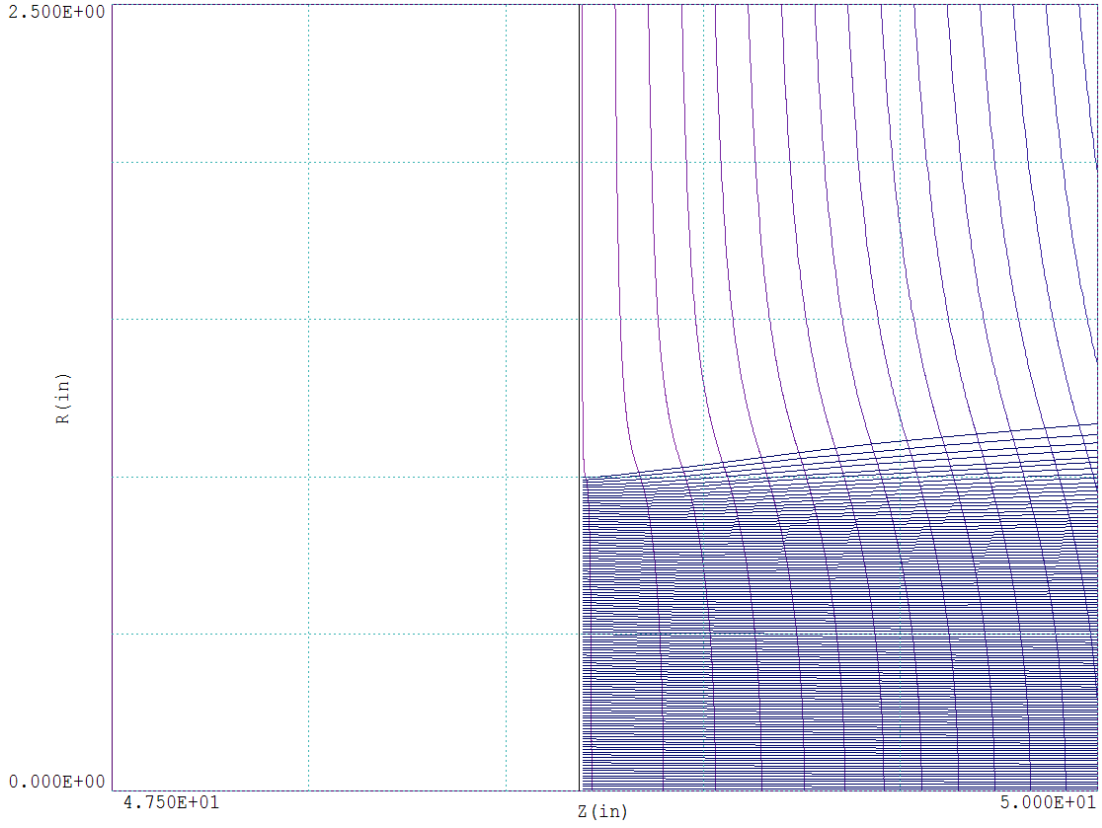

Figure 5: Electron beam extracted from a 2-inch diameter, space-charge limited emitter that is flush with the flat surface of the Axis-I cathode shroud. Simulation of this geometry produced 2.1 kA with V_{AK}=3.8 MV. N. B. The density of rays is not equivalent to current density because the rays do not carry equal currents.

The equipotentials in Fig. 5 clearly show the space-charge depression on axis near the emitter. The reduced electric field in the center extracts a lower current density, producing a beam with a higher current density at the edge than at the center. This effect, clearly seen in a plot of current density across the emission face (Fig. 6), is often called "edge emission," even though there is no field enhancement by the edge for this ideal case.

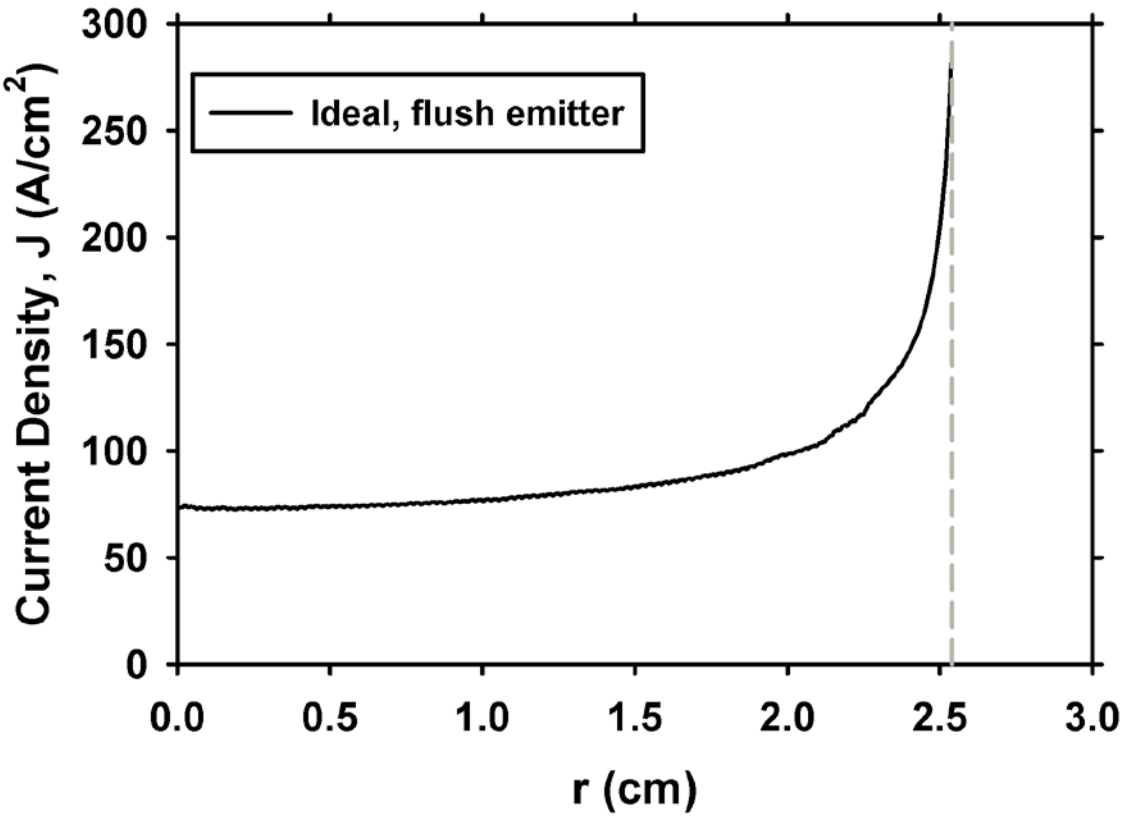

Figure 6: Current density across the ideal, flush emitter shown in Fig. 5. The total current is 2.1 kA with V_{AK}=3.8 MV. The outer edge of the 2-inch diameter cathode is shown by the dashed line.

The hollowing of the beam from an ideal flush cathode is exacerbated by the as-built Axis-I cathode, because the as-built cathode has an edge that enhances the field and causes true edge emission in addition to the space-charge suppression near the center. Figure 7 shows the space-charge limited beam extracted from an as-built cathode surface that is flush with V_{AK}=3.8 MV. The equipotentials in this figure clearly show the space-charge depression on axis near the emitter, as well as the enhancement at the cathode edge. This simulation produced 2.25 kA, about 150 A more than the ideal flush emitter. The extra current comes from the extra area wrapping around the edge, and the enhancement of the field near there.

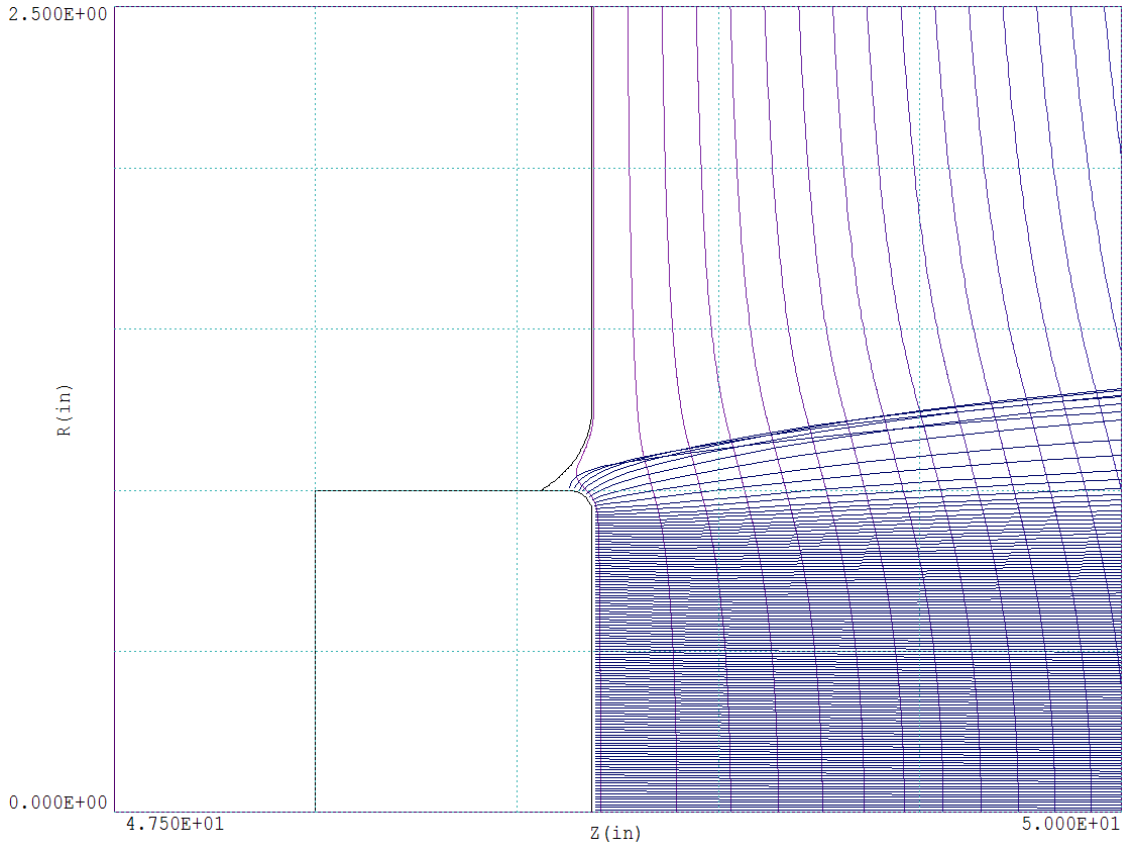

Figure 7: Electron beam extracted from the as-built 2-inch diameter cathode positioned to be flush with the flat surface of the Axis-I cathode shroud. Simulation of this geometry produces 2.25 kA with V_{AK}=3.8 MV. N. B. The density of rays is not equivalent to current density, because the rays do not carry equal currents.

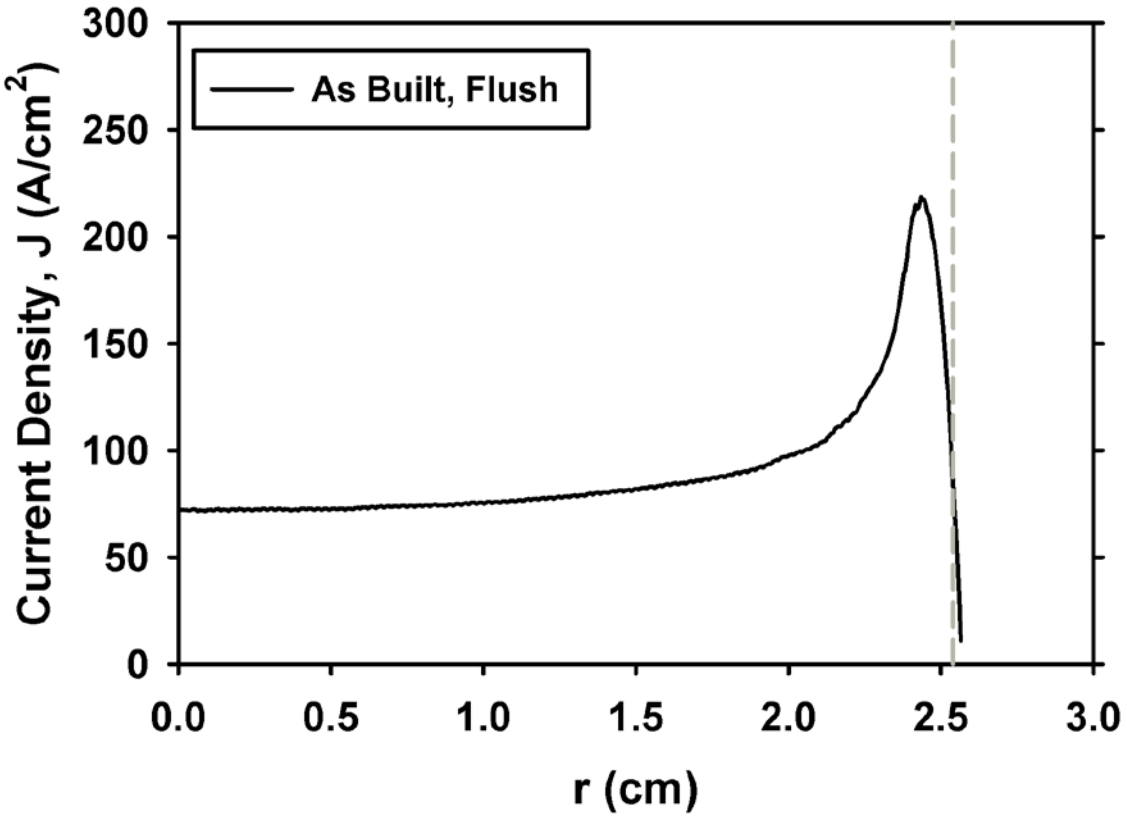

Figure 8: Current density across the as-built, flush emitter shown in Fig. 7. The total current is 2.25 kA with V_{AK}=3.8-MV. The outer edge of the 2-inch diameter cathode is shown by the dashed line. N. B. The plotted current density is over the entire emission surface, which wraps around the cathode edge as shown in Fig. 7.

Since the cathode plasma produced by explosive emission process rapidly expands [6] the location of the emission surface is not coincident with the surface of the velvet. Recessing the cathode reduces the potential and field at the velvet, so in the simulations I recessed the cathode until the current was the nominal value (1.74 kA) used in XTR envelope code simulations with 3.8-MV AK voltage. Figure 9 shows the simulated current as a function of the depth of the surface. Recessing the as-built cathode model into the shroud to a depth of 2-mm gave the nominal 1.75-kA current at V_{AK}=3.8 MV. The sensitivity of current reduction (~252 A/mm) by recessing the cathode is greater than planar diode scaling (Jd^2 = constant), because of the further reduction of potential in a hole. I presume that the difference between the 2-mm cathode depth in the simulation and the measured depth (~2.5 mm) of the actual cathode is likely due to the emitting plasma thickness.

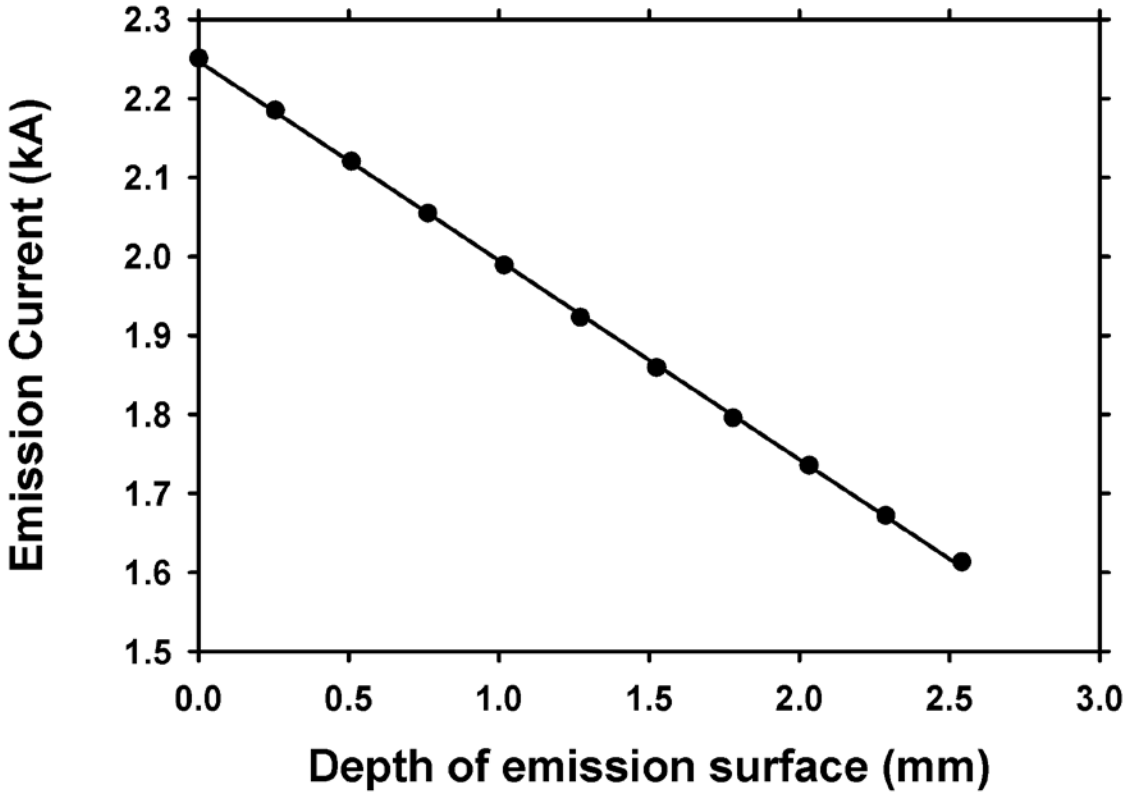

Figure 9: Simulated current emitted by the model of the as-built cathode as a function of the depth of retraction below the shroud surface. The sensitivity is the slope of the least square fit line: -252 A/mm.

In addition to reducing the current, recessing the cathode has the Pierce-like effect of reducing the edge emission by flattening the equipotentials in the presence of beam space charge. In fact, this accounts for much of the current reduction. Figure 10 shows the beam produced by the recessed cathode, and the current density is plotted in Fig. 11. Finally, the current density for the flush and recessed cathodes is compared in Fig. 12, showing that the reduction in current is largely due to suppression of edge emission.

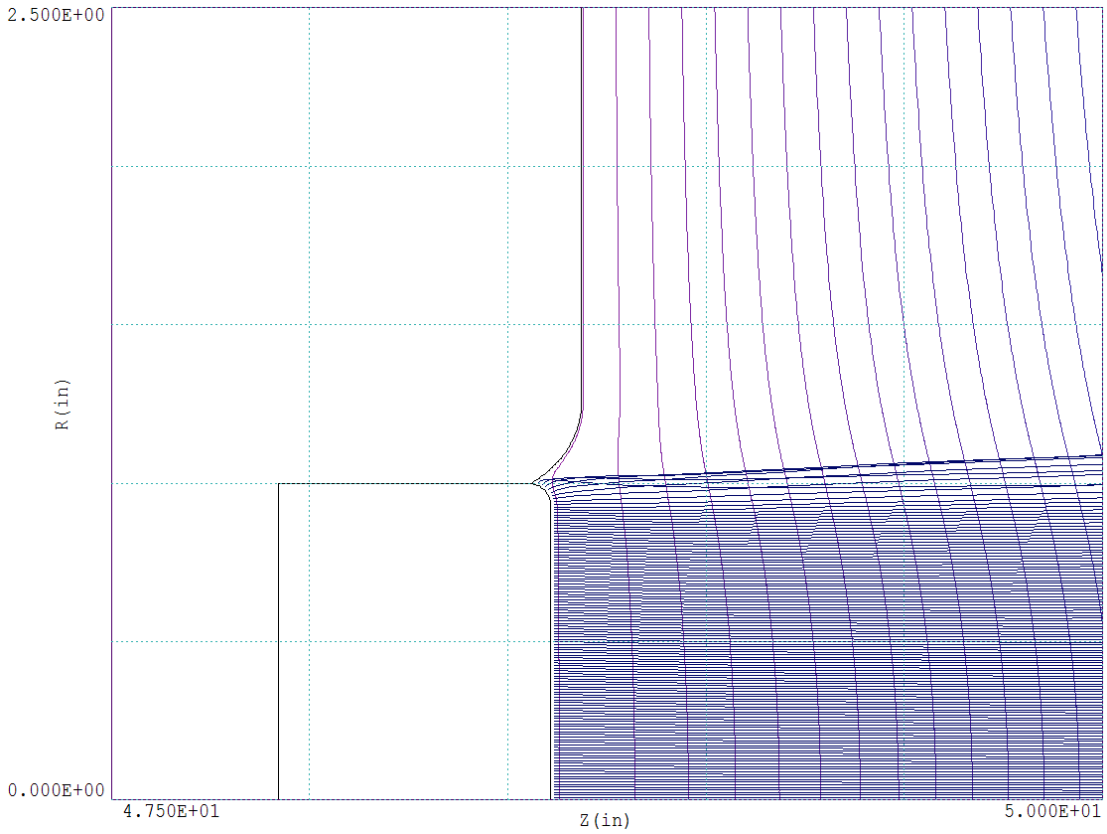

Figure 10: Electron beam extracted from the as-built 2-inch diameter cathode retracted 2 mm below the flat surface of the Axis-I cathode shroud. Simulation of this geometry produces 1.75 kA V_{AK}=3.8-MV. N. B. The density of rays is not equivalent to current density, because the rays do not carry equal currents.

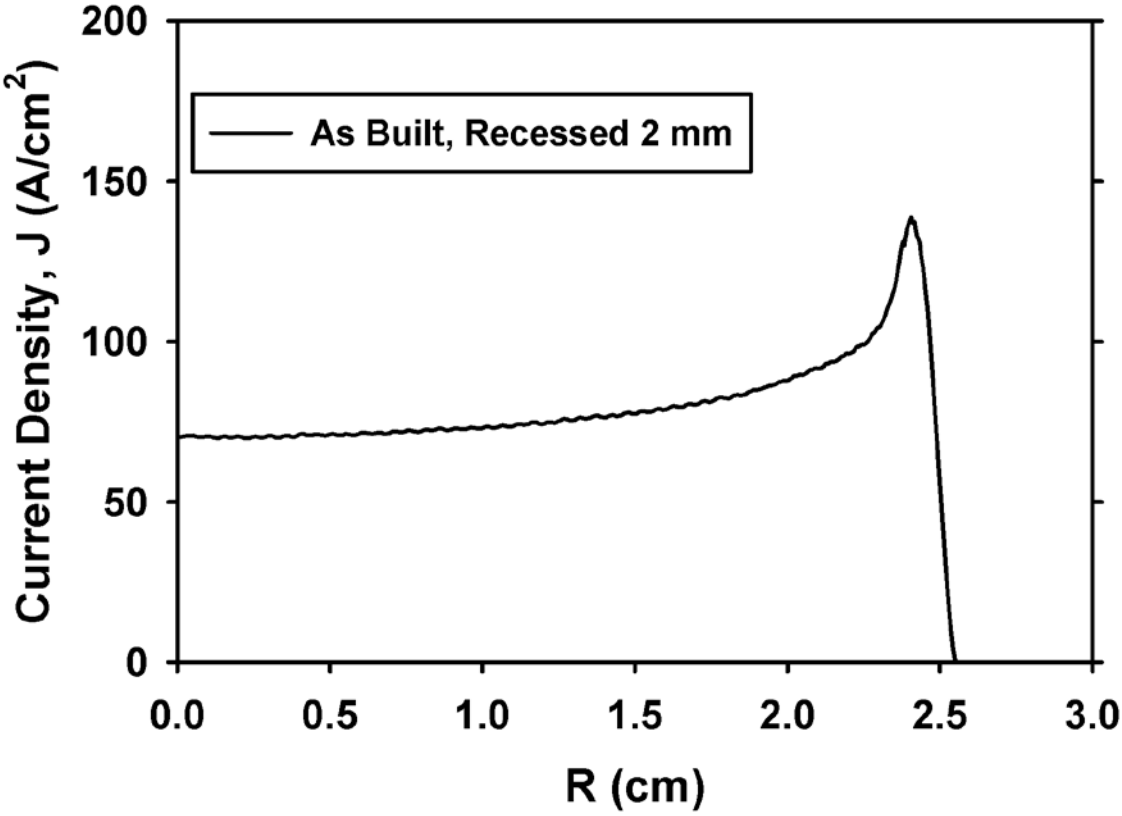

Figure 11: Current density across the as-built, recessed emitter shown in Fig. 10. The total current is 1.75 kA at V_{AK}=3.8 MV. The outer edge of the 2-inch diameter cathode is shown by the dashed line. N. B. The plotted current density is over the entire emission surface, which partially wraps around the cathode edge as shown in Fig. 10.

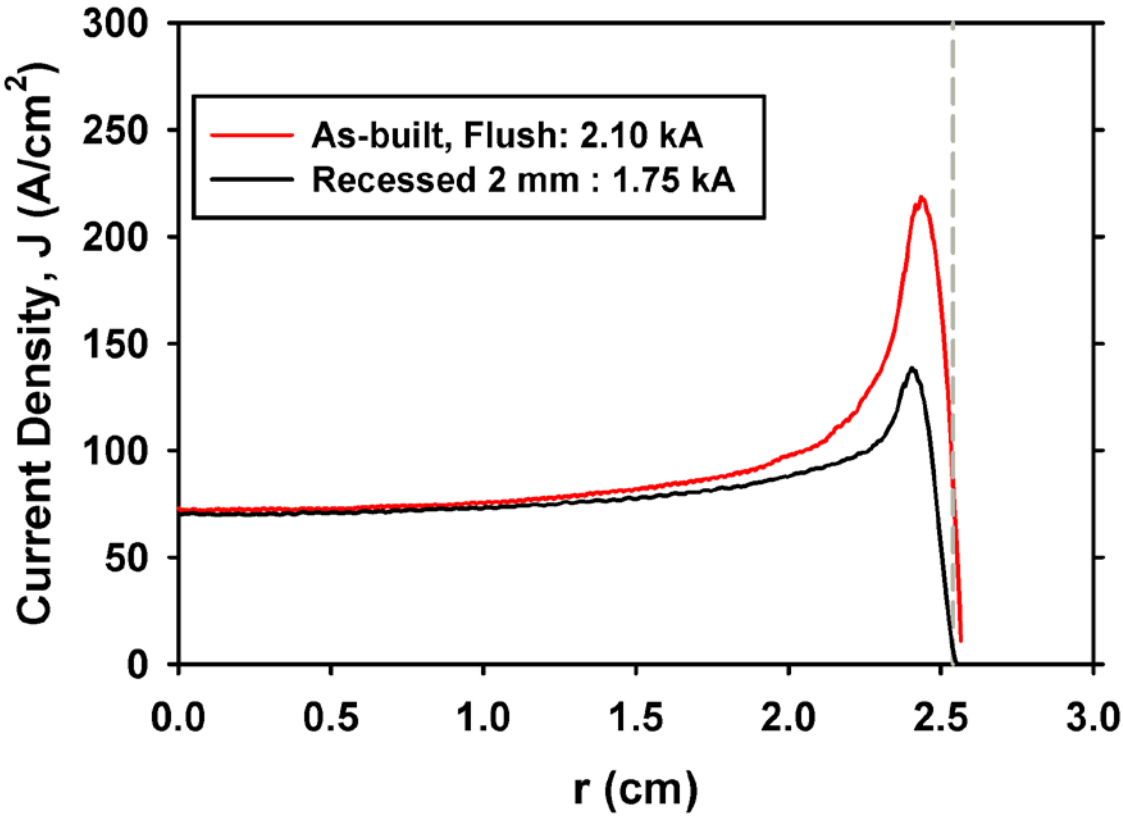

Figure 12: Comparison of current density distributions for as-built cathodes flush with surface (red curve) and retracted by 2 mm (black curve). The outer edge of the 2-inch diameter cathode is shown by the dashed line. N. B. The plotted current density is over the entire emission surface, which partially wraps around the cathode edge as shown in Fig. 7 and Fig. 10.

II. Comparison with Experimental Data

I-V Scaling

Validation of simulations must include comparison of results to experimental data over as wide a range of variables as possible. I compared these simulations to experimental data acquired on September 29, 2010 and October 18, 2010. I analyzed the data from 20 shots on these two days with the wid_beam.pro analysis program [10], using BPM02 data for the beam current. These 20 shots covered a range of diode voltages from 2.12 MV to 3.81 MV, and included the shot that radiographed hydrotest 3648. I used the average voltage and current reported by wid_beam.pro to compare with the TRAK simulations. This comparison is shown in Fig. 12.

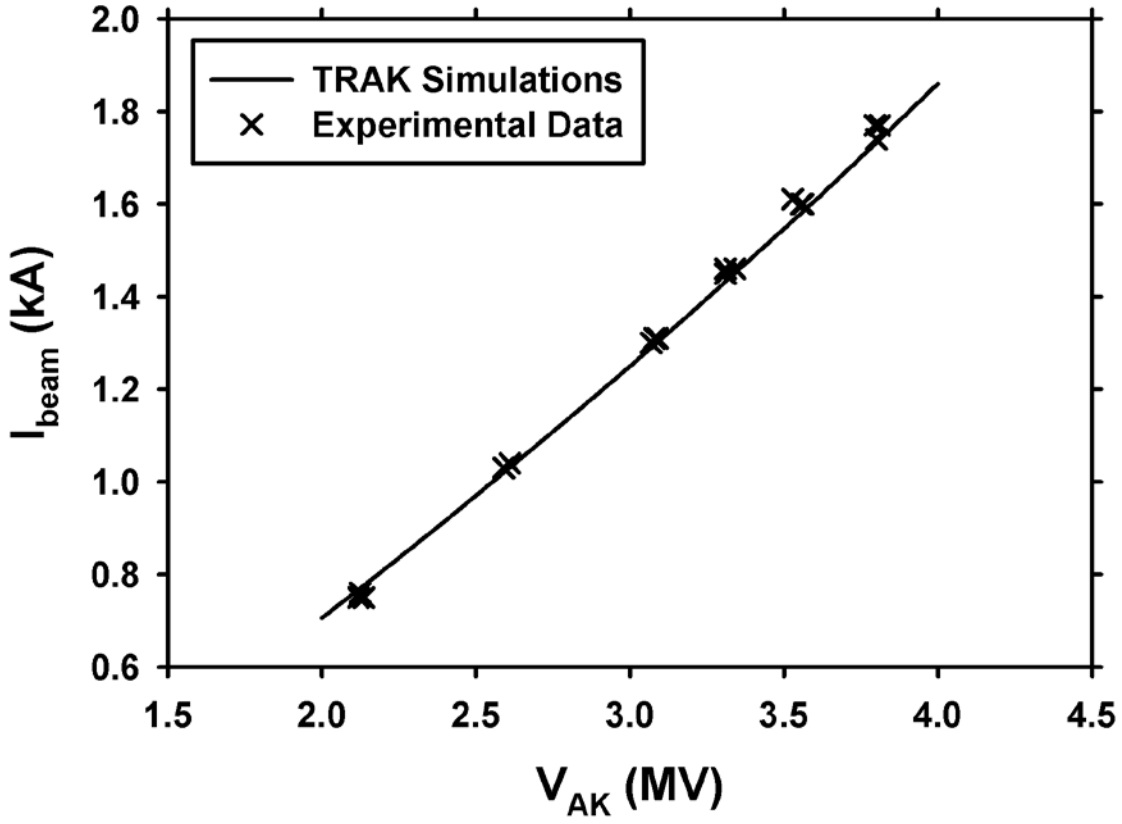

Figure 13: Comparison of experimental data with TRAK simulations of the Axis-I diode.

Retraction depth scaling

The sensitivity of the current to retraction depth predicted by the simulations (~252 A/mm, Fig. 9) should be compared to data available for the 2-inch cathode. Experimental validation of this prediction is an important test of the accuracy of the simulations.

Beam size and convergence

TRAK calculates rms beam parameters at specified locations directly from the distribution of particle trajectories. TRAK also calculates the beam current distribution from the self magnetic field, and I used this distribution to calculate the rms radius as a check on the rms radius from the trajectories. The TRAK values were obtained at the initial position of the XTR envelope code integration, in order to compare with the XTR initial conditions, which were derived from experimental data [11]. All of these are compared in Table I for the case of 1.75 kA at 3.8 MV. Derived parameters are in parentheses. The agreement between the beam parameters predicted by TRAK and those used for XTR initial conditions is poor.

Source			XTR	TRAK	TRAK
method				particle	current
parameter	**derivation**	**units**			
R_0	$=\sqrt{2}R_{rms}$	cm	2.357	(3.026)	(3.09)
R_{rms}	$=R_0/\sqrt{2}$	cm	(1.667)	2.140	2.185
R_0' *		mr	-14.76		
R_{rms}' *		mr		18.36	
ε		pi-cm-rad		0.00245	n/a
ε_n	$=\beta\gamma\,\varepsilon$	pi-cm-rad	0.0850	(0.0205)	n/a

*The sign convention for beam convergence in TRAK is opposite the convention used in XTR. That is, R' is negative in XTR for a converging beam, but positive in TRAK.

III. Discussion

I-V Scaling

Validation of simulations should also include comparison of results with exact analytic solutions whenever possible. As Irving Langmuir first showed for non-relativistic diodes, the dependence of current on AK voltage is independent of the diode geometry, so one only needs the planar diode solution to establish the I-V scaling law [8]. That is, for all non-relativistic diodes $I \propto V^{3/2}$, with a proportionality constant determined by the specific geometry. Langmuir's ansatz can be extended to the relativistic diode regime, so all geometries of relativistic diodes should have the same scaling of current as a function of AK voltage. To establish this I-V scaling I rely on the exact relativistic planar diode theory derived by Jory and Trivelpiece [9], referred to herein as JT. For comparison with the experimental data and TRAK simulations, I numerically integrated the JT equations to avoid dealing with the elliptic integrals in the JT analytic results. Under the Langmuir similarity hypothesis one then expects the simulations to scale as the analytic planar diode theory; $I_{TR}(V) = gI_{JT}(V)$ where I_{TR} is the TRAK simulated current, I_{JT} is the Jory-Trivelpiece planar solution, and g_0 is a geometry factor. The comparison is shown in Fig. 14.

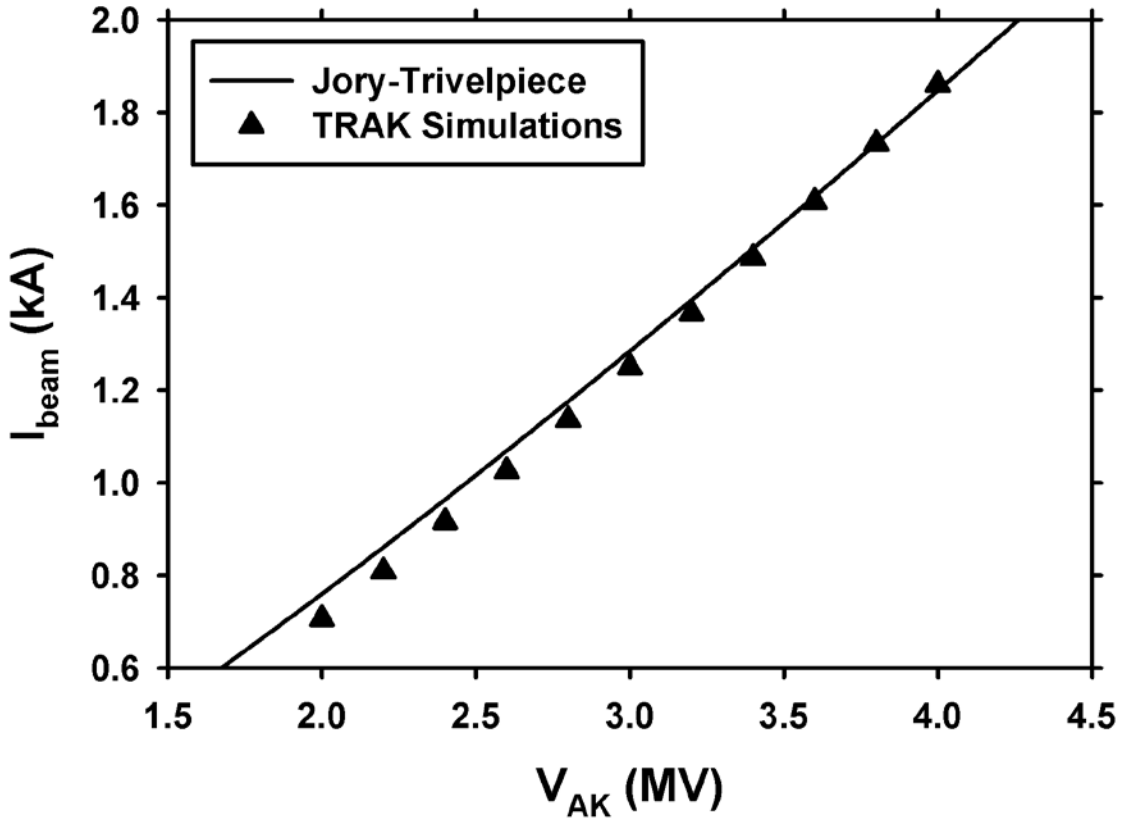

Figure 14: Comparison of Jory-Trivelpiece Theory with TRAK simulations. The theory was normalized to the simulations for 3.8 MV.

Although the agreement appears poor in Fig. 14, using JT theory to predict the current in these simulations would only have resulted in an rms error of ~38 A, or ~ 2%. My experience with other relativistic diodes, including the Axis-II diode, has always shown good agreement with JT, so this discrepancy is worth further investigation. My initial hypothesis was that the disagreement is entirely the result of the hollow beam resulting from edge emission (Fig. 11). However, a series of simulations to produce a beam with a more uniform profile did not fit the JT analytic result any better than the hollow beam simulations, so the cause of the discrepancy must lie elsewhere.

In practice, it is useful to have a rule of thumb for I-V scaling. It has long been known that a power law scaling fits the Axis-I data [11], so I fit a power law to the TRAK simulations. The result, shown in Fig. 15, is $I = 0.271 V_{AK}^{1.3898}$, so a 1.4 power law might be adequate for most applications. Moreover, an effective perveance $P_{eff} \equiv I / V^{1.4}$ where current and voltage are measured values, can be an excellent diagnostic of diode health, especially if plotted as a function of time during the pulse.

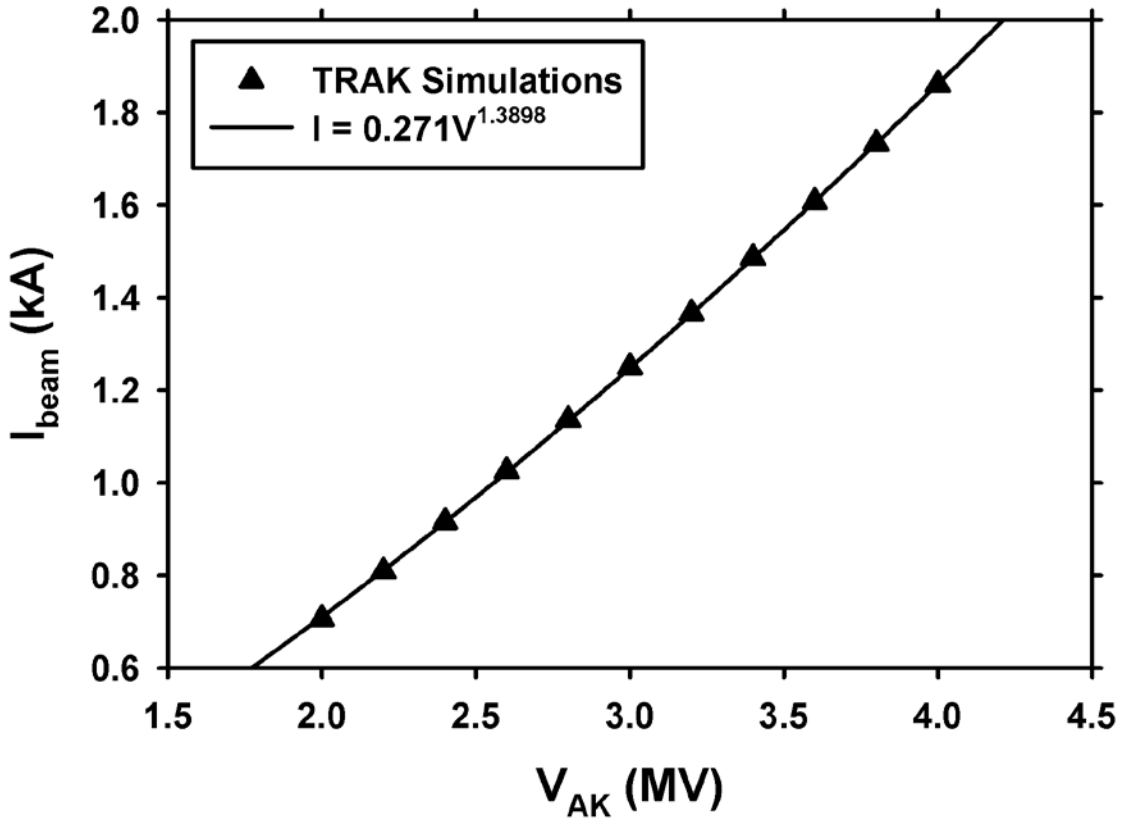

Figure 15: Power law fit to the TRAK simulations shown in Fig. 14.

Diode closure (impedance collapse)

Although apparent closure speeds as high as 6 cm/μs have been reported for cold-cathode diodes, these were observed in high current density diodes with metallic anodes, and may be attributed to anode plasma closure, ion emission, and transition to bipolar flow. Therefore, much lower closure speeds should apply to the Axis-I foil-less diode with its low current density.

In ref. [6] Bruce Miller proposed a scaling of closure speed for velvet cathodes $v = KJ^{1/3}$, where the scaling constant depends only on the properties of the velvet. The closure speeds in the experiments of ref. [6] were less than 2.5 mm/μs at current densities less than 12.4 A/cm^2. Presuming that the Axis-I velvet is not much different than the types used in ref. [6], this scaling would predict a closure speed less than 4.8 mm/μs at 1.75 kA (3.8 MV). Based on the current sensitivity predicted by TRAK (Fig. 9), this closure speed would result in a ~1.2-kA/μs rate of increase in current, which is only about 72 A at the end of the Axis-I 60-ns pulse.

Diode closure was observed in the PIVAIR injector at CESTA (Fr.), which is a duplicate of the Axis-1 injector, and also used a velvet cathode [12]. For example, Fig. 15 shows the current measured from the PIVAIR diode. Time-resolved magnetic spectrometer measurements of the beam energy at the diode exit determined that the 3.52-MV AK voltage was constant to within +/-0.74% over the pulse flattop, so the current increase shown in Fig. 16 is a clear indication of diode closure. The closure rate indicated by the current rise is ~1.8 kA/μs, as depicted by the red line I added to Fig. 16. This is substantially faster than predicted by these simulations of the Axis-I 2-inch cathode, and may be due to the larger cathode on PIVAIR, or to the details of how it was recessed.

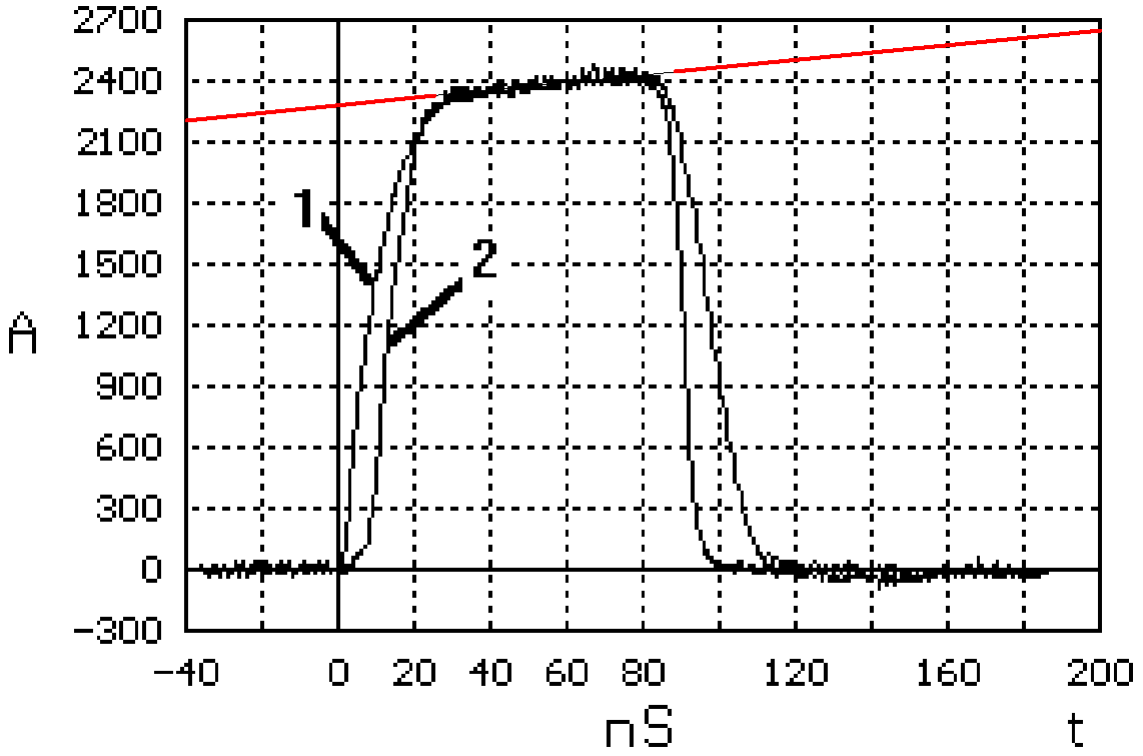

Fig. 16: Beam current measured on PIVAIR at injector output (1) and after 16 accelerator cells (2) [12]. I added the red line to clearly show the ~1.8-kA/μs diode closure rate.

IV. Conclusions

Current-voltage scaling from finite element simulations of the DARHT Axis-I diode is in good agreement with experimental data for the standard 2-inch cathode, lending credence to the simulations. Neither the simulations nor the data agree with the analytic theory to better than 2-3%. The beam parameters predicted by the simulation disagree with the initial values used in XTR envelope calculations. Cathode plasma closure speeds predicted by scaling a phenomenological theory to these simulations were evident in

measurements on the PIVAIR injector, which is a duplicate of the DARHT Axis-I injector.

Acknowledgements

I want to acknowledge interesting and illuminating discussions with my WX-5 colleagues, in particular Dave Moir and Trent McCuistian. This work was supported by the US National Nuclear Security Agency and the US Department of Energy under contract W-7405-ENG-36.

References

[1] Stanley Humphries Jr., "TRAK – Charged particle tracking in electric and magnetic fields," in Computational Accelerator Physics, R. Ryne Ed., New York: American Institute of Physics, 1994, pp. 597-601.

[2] Stanley Humphries Jr., *Field solutions on computers*, (CRC Press Boca Raton, FL 1997) and www.fieldp.com

[3] Thomas P. Hughes, David C. Moir and Paul W. Allison, "Beam injector and transport calculations for ITS," in Proc. 1995 Part. Accel. Conf., 1995, pp. 1207-1209.

[4] G. A. Mesyats and D. I. Prosurovsky, *Pulsed Electrical Discharge in Vacuum*, (Springer-Verlag, Berlin 1989)

[5] R. J. Adler, et al., "Improved electron emission by use of a cloth fiber cathode," Rev. Sci. Instrum. 56, 1985, pp. 766-767

[6] R. B. Miller, "Mechanism of explosive electron emission for dielectric fiber (velvet) cathodes," J. Appl. Phys. 84, 1998, pp. 3880 -3389

[7] Stanley Humphries Jr., *Charged particle beams*, (Wiley, NY, NY 1990), p. 263 et seq.

[8] Irving Langmuir and K. T. Compton, "Electrical discharges in gases II. Fundamental phenomena in electrical discharges," Rev. Mod. Phys. 3, 1931, pp 191- 258

[9] H. R. Jory and A. W. Trivelpiece, "Exact relativistic solution for the one-dimensional diode," J. Appl. Phys. 49, 1969, pp. 3924-3926

[10] G. W. Sullivan and D. C. Moir,

[11] D. C. Moir, Private Communication

[12] P. Eyharts, et al., "Beam transport and characterization on AIRIX prototype at CESTA," PAC97, p. 1257